JOURNAL OF CATALYSIS 113, 185–192 (1988)

A Temperature-Programmed Desorption Study of NO on Rh Particles Supported on α-Al_2O_3{0001}[1]

E. I. ALTMAN AND R. J. GORTE

Department of Chemical Engineering, University of Pennsylvania, Philadelphia, Pennsylvania 19104

Received February 1, 1988; revised April 11, 1988

The adsorption and dissociation of NO on Rh/α-Al_2O_3{0001} was studied as a function of Rh particle size using temperature-programmed desorption (TPD). Samples were prepared by vapor depositing varying amounts of Rh onto the sapphire crystal at 300 K. Auger electron spectroscopy indicated that the Rh formed three-dimensional particles under these conditions, and an average Rh particle diameter was estimated from the CO adsorption uptake and the amount of metal deposited. On particles larger than 5 nm, the TPD results were essentially identical to those for Rh(111) and Rh(110), with approximately 60 to 80% of the NO dissociating. Molecular NO desorbed in a peak centered at 440 K, and N_2 desorbed in peaks at 460, 550, and above 600 K. For smaller Rh particles, the molecular desorption peaks and the fraction of NO dissociating remained unaffected; however, significant changes were observed in the N_2 desorption features. The N_2 feature at 460 K, which has been assigned to a reaction between NO and N atoms, disappears for very small particles and the N atom recombination peak at 550 K shifts above 600 K. By comparing these results to those obtained for various single crystals, we conclude that changes observed with particle size are related to site geometry; however, the desorption rates from small particles cannot be considered to be a simple sum of the rates for different single crystals. It is shown that these changes in the N_2 desorption rates with particle size may be responsible for observed structure sensitivity in NO reduction by CO.

INTRODUCTION

While many of the detailed investigations of adsorption properties on catalytic metals have been carried out using metal single crystals, most practical catalysts consist of small metal particles supported on an oxide substrate such as alumina. In order to compare the catalytic properties of these very different catalysts, we have been investigating the adsorption properties of small Pt and Rh particles on flat alumina substrates using techniques normally used for single crystals and comparing the results to similar measurements on single-crystal surfaces (*1–3*). These model-supported catalysts allow the use of surface spectroscopies, such as Auger electron spectroscopy (AES), and simplify the interpretation of temperature-programmed desorption (TPD) results by eliminating complications due to diffusion and readsorption (*4, 5*). A very interesting observation from this work is that desorption of CO is strongly affected by both particle size and crystal plane on Pt, while TPD curves measured for CO on Rh are only weakly dependent on these properties. Furthermore, the close similarities between desorption states observed for CO on Pt and Rh particles and desorption states for CO from Pt and Rh crystals suggest that the surfaces of the metal particles can be thought of as a sum of single-crystal surfaces (*24*). This is also consistent with kinetic studies which have shown that reactions which depend on metal particle size also show a rate dependence on crystallographic orientation in single-crystal studies (*6–9*).

To further test the idea that the crystallographic orientation of the sites on sup-

[1] This work was supported by the Department of Energy, Basic Energy Sciences, under Grant DE-FG03-85-ER13350. Some facilities were provided by the NSF, MRL Program, under Grant DMR 82-16718.

0021-9517/88 $3.00

ported metal particles is important in determining the adsorption and reaction properties, we have extended our previous work by examining the adsorption of NO on Rh. There are several reasons for examining this adsorption system. First, NO can adsorb both molecularly and dissociatively adding a degree of complexity not present in CO adsorption. Second, the reduction of NO over a Rh catalyst is of practical importance in the automotive catalytic converter. Recently it was shown that specific rates and activation energies for NO reduction by CO are considerably different on a Rh(111) crystal and a supported Rh/Al_2O_3 catalyst (*10*). Structure sensitivity of NO reduction was also suggested by Hecker and Breneman (*11*) who reported that the specific rates and activation energies also change with particle size. Furthermore, some variations are found in the TPD curves for NO on Rh crystals, with Rh(100) displaying a N_2 desorption peak 100 K higher than Rh(111) or Rh(110) (*12–17*).

In this paper, we will show that NO TPD does depend on particle size and that the desorption behavior of small particles cannot be explained by considering the particles to be a sum of simple crystal planes. While temperatures for the desorption of molecular NO and the fraction of NO dissociating during the TPD experiments are not strong functions of particle size, we observe a significant increase in the peak temperature for N_2 with decreasing particle size. In addition, a N_2 desorption feature which has been assigned to a reaction between adsorbed NO and N becomes negligible for very small particles (*10, 13, 15, 18*). Finally, we have used a kinetic model of the NO–CO reaction developed for Rh(111) to show that these changes in the desorption properties may be responsible for the observed structure sensitivity of this reaction on Rh.

EXPERIMENTAL

The experimental equipment and procedures have been described previously (*1–3*). Briefly, all experiments were performed in an ultrahigh vacuum chamber equipped with a cylindrical mirror analyzer for Auger electron spectroscopy, a quadrupole mass spectrometer, an ion gun for sample cleaning, a resistively heated Rh evaporation source, and a calibrated film thickness monitor to measure Rh evaporation rates. The mass spectrometer was interfaced to a computer for multiplexing and data acquisition. An α-Al_2O_3{0001} crystal with a 300-nm gold film on the back side was used as the substrate. The crystal was heated by passing current through Ta wires clamped to the back with insulating ceramic posts. Temperatures were measured with a Chromel–Alumel thermocouple pressed between the crystal and one of the ceramic posts, and heating rates were maintained at 7 K/sec in all of the experiments reported in this paper. In order to obtain saturation exposures of various gases, we placed the sample in front of a directed doser so that the sample could be exposed to large gas fluxes without substantially increasing the base pressure of the vacuum system. Exposures in front of the doser were estimated by comparing TPD curves obtained with the sample in front of the doser and turned away from the doser. We used exposures of approximately 5 L for NO and CO and 25 L for O_2 for saturation (1 Langmuir of NO = 3.7×10^{14} molecules/cm^2).

Auger spectra taken prior to Rh evaporation showed Al and O, with only Ar and very small amounts of N as impurities. Following Rh deposition at room temperature, the only new Auger features were due to Rh, and examination of the AES peak intensities as a function of metal coverage indicated that three-dimensional particles were formed under these conditions (*3*). We reported previously that CO TPD areas increased after exposing the sample to NO. However, NO TPD taken immediately after depositing Rh onto the substrate at room temperature followed by exposure to NO were identical to subsequent TPD measurements. The average particle diameter was

estimated from the amount of the metal deposited as measured by the film thickness monitor and the amount of CO adsorbed at saturation as measured by TPD. Since the area under the saturation TPD curve for CO did not change for metal coverages above 5×10^{15} atoms/cm^2, we took this metal coverage to correspond to a continuous film for purposes of calculating particle size. For these calculations, we assumed a constant adsorption stoichiometry for CO, independent of particle size, and spherically shaped particles. These assumptions are discussed in more detail elsewhere (*1*). The system was relatively more sensitive to N_2 than to NO; therefore, the percentage of NO that dissociated could not be determined by directly comparing the TPD areas of N_2 and NO. Estimation of the amount of NO dissociation will be discussed later.

RESULTS

The TPD curves obtained for saturation coverages of NO for a range of Rh particle sizes from 2.6 nm up to a continuous film are shown in Fig. 1. For all particle sizes studied, a substantial fraction of the NO dissociated during the temperature ramp. While N_2 desorption curves are shown, the oxygen formed by NO dissociation had to be removed by titrating the surface with CO since the sample could not be heated to the desorption temperatures for oxygen on Rh. The fraction of NO which dissociated during TPD appeared to decrease slightly with decreasing particle size but remained between 60 and 80% for all particles. This dissociation fraction is in the same range reported for single crystals of Rh (*12–17*). Also, desorption features for the unreacted NO remain reasonably constant. Most of the NO desorbed in a peak centered at 440 K, with some NO desorbing at 410 K. These results, too, are similar to those obtained on single crystals, where desorption features for molecular NO are essentially independent of crystal plane (*12–17*). In single-crystal studies, the desorption peak at 440 K has been identified as desorption

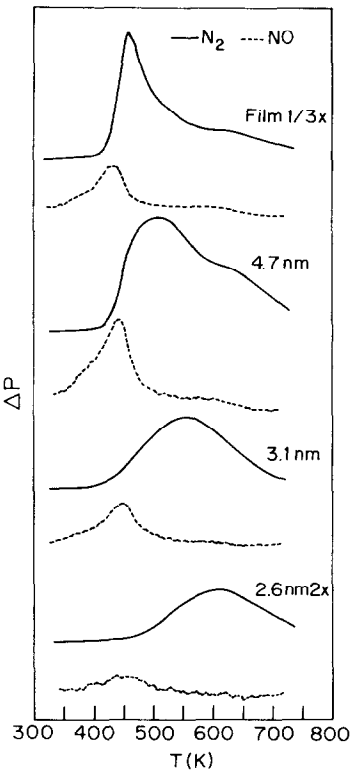

FIG. 1. TPD of NO at saturation coverages for different Rh particle sizes. The solid lines are for N_2 and the dashed lines for NO. From top to bottom, the Rh coverages were 5×10^{15}, 2×10^{15}, 1×10^{15}, and 3.5×10^{14} Rh atoms/cm^2.

from a clean Rh surface, while an additional peak at 410 K is observed when NO is coadsorbed with its dissociation products or O_2 (*19, 20*). This similarity in the adsorption of molecular NO on bulk Rh and small Rh particles can also be seen by comparing vibrational spectra for supported Rh catalysts and Rh single crystals. Infrared spectroscopy of Rh/SiO_2 and HREELS of Rh(111) exhibit essentially identical NO vibrational frequencies (*19–21*). Although we did not monitor NO dissociation spectroscopically, the fact that NO molecular desorption features, the amount of NO dissociation, and the NO vibrational frequencies are similar for supported Rh particles and Rh single crystals strongly implies that NO dissociation is also similar on Rh particles and Rh crystals.

The main differences found in the TPD curves as a function of particle size occurred in the N_2 desorption features. For the continuous film, most N_2 desorbs in peaks centered at 460 and 550 K, with a smaller amount desorbing in a feature above 600 K. The peaks at 460 and 550 K and their relative intensities are similar to desorption results for several Rh single crystals, including Rh(111) and Rh(110) (*13, 14*), while N_2 desorption occurs in peaks at 460 and 700 K on Rh(100) (*15*). The much sharper feature at 460 K has been assigned to N_2 formed by a reaction of adsorbed, molecular NO with nitrogen atoms and is observed on all of the bulk Rh samples which have been reported in the literature (*12–18*). The features at 550 K and higher temperatures must be due to the recombination of nitrogen atoms since several spectroscopic studies have shown that all NO has either desorbed or dissociated below these temperatures (*14, 15, 19*). When the particle size is reduced, the relative amount of N_2 desorbing above 600 K increases significantly. The other change observed is that the relative intensity of the peak at 460 K decreases dramatically and is not observed at all on the smallest particles. This implies that the removal of N_2 from the surface by the reaction of molecular NO with nitrogen atoms becomes unimportant on very small particles. Both the disappearance of the 460-K N_2 peak and the increase in temperature of the nitrogen recombination peak imply that N atoms adsorbed on small Rh particles are considerably less reactive than N atoms on Rh crystals.

It is interesting to compare our results to those of Chin and Bell who reported TPD curves for NO on a porous Rh/SiO_2 catalyst with a dispersion of 16.4% (average particle diameter of ~5 nm) (*22*). Their results were very similar to ours for particles of this size except that they reported 97% dissociation of NO and observed the formation of some N_2O. These differences can be easily explained by readsorption effects which will almost certainly be important for molecular NO desorbing from a porous Rh catalyst (*4, 5*). Therefore, the results of Chin and Bell support our conclusions for particles of this size range.

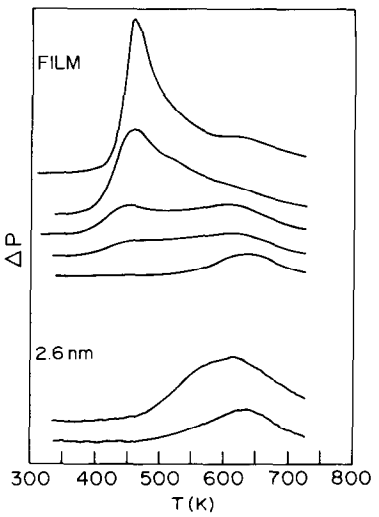

FIG. 2. N_2 desorption as a function of NO coverage for 2.6-nm Rh particles and a Rh film.

We also examined the effect of initial NO coverage on N_2 desorption, with results shown in Fig. 2 for the continuous film and for the smallest particles. From this, it can be seen that the high-temperature peak fills first, followed by the lower-temperature peaks which appear to fill together. Similar results are observed for Rh(111) (*13*). While the N_2 peaks at 550 and 615 K shift to slightly lower temperatures as the coverage is increased, as should be anticipated for second-order processes, the two features do appear to be distinct. For 2.6-nm particles, a small shift in desorption temperature is also observed as the coverage is increased. Again, this is similar to the behavior observed for the high-temperature N_2 peak on Rh(100) (*15, 16*).

The effect of coadsorbed oxygen on NO adsorption was also studied. In Fig. 3, the TPD curves for NO on the clean and O_2-saturated surfaces are shown for the film and for the 3.1-nm particles. In agreement with coadsorption studies on Rh(111)

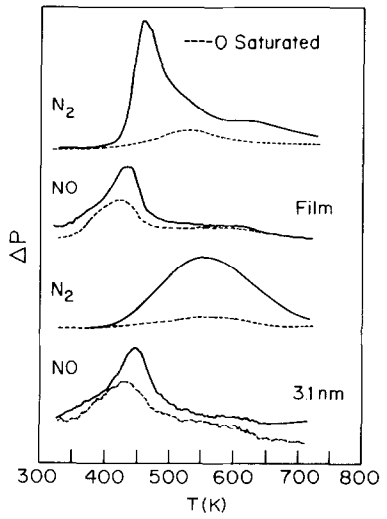

FIG. 3. TPD for saturation NO coverages from clean (—) and oxygen-saturated (---) Rh/α-Al_2O_3 surfaces. Results are shown for 3.1-nm particles and a Rh film.

(*13*, *19*), the N_2 desorption peaks are reduced by more than 80%, demonstrating that dissociation of NO is blocked by the adsorbed oxygen for both small and large particles. While molecular NO desorption is still observed, the amount of NO is decreased and the peak is shifted to lower temperatures. Root *et al.* (*13*) reported similar results and were able to resolve the NO desorption curve into two peaks at 410 and 460 K, with all of the NO desorbing from the state at 410 K on the oxygen saturated surface. To determine whether oxygen preferentially removed only certain sites, we also examined the effect of smaller oxygen coverages, as shown in Fig. 4 for intermediate-sized particles in which all three N_2 desorption states are easily observable. In these experiments, successive TPD were taken following exposures to a saturation coverage of NO without removing the adsorbed oxygen between the measurements. These results show that the high-temperature peak at 615 K is attenuated more quickly at low-oxygen coverages than the peaks at 460 and 550 K. Adsorbed oxygen either blocks the sites responsible for this peak preferentially or shifts the desorption peak to coincide with the other peaks. The peaks at 460 and 550 K are also better resolved in the presence of adsorbed oxygen, possibly due to small changes in their relative populations or small temperature shifts in the two peaks.

As discussed earlier, we were unable to heat our sample to temperatures high enough to desorb O_2 from the Rh particles. Following each of the TPD measurements, the surface was exposed to CO to remove the oxygen by the reaction to form CO_2. Titration with CO was also used to determine the relative amount of oxygen remaining on the Rh surface following TPD of NO and, indirectly, to estimate the fraction of NO which dissociated during TPD. In these experiments, the Rh was first exposed to saturation coverages of O_2 or NO at room temperature. For the NO-saturated case, the sample was then ramped to temperatures above the N_2 desorption peaks and allowed to cool back to room temperature. The oxygen coverage was estimated by exposing the sample to 1.5 L of CO and performing TPD measurements. The results for O_2 and NO adsorption on the 4.7-nm

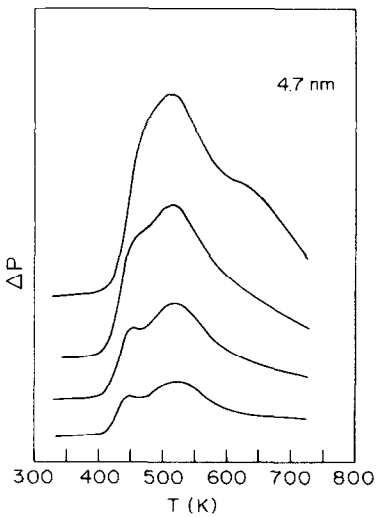

FIG. 4. Successive TPD curves for N_2 following repeated saturation coverages of NO on 4.7-nm particles. The changes are due to the buildup of adsorbed oxygen formed by the dissociation.

particles are shown in Figs. 5a and 5b, respectively. The main point of interest in these coadsorption results is that the amount of CO_2 formed by the oxygen from the NO-covered surface is very close to 50% of that formed from the O_2-saturated surface. This value of 50% was found to be independent of particle size in our measurements. Assuming that the amount of CO_2 formed in this procedure is linearly dependent on the initial oxygen coverage (an approximation which successive CO adsorption–titration measurements validate) and that the adsorption stoichiometries for oxygen on Rh (~0.83 atoms/Rh) (*13*) and NO on Rh (0.62–0.65 molecules/Rh) (*13, 15, 16*) are independent of surface geometry, we calculate that the fraction of NO which dissociates in TPD is between 60 and 80%, very close to the fraction reported in studies on single crystals (*12–17*). Desorption temperatures for the CO_2 formed by this reaction are also close to those observed on Rh(111).

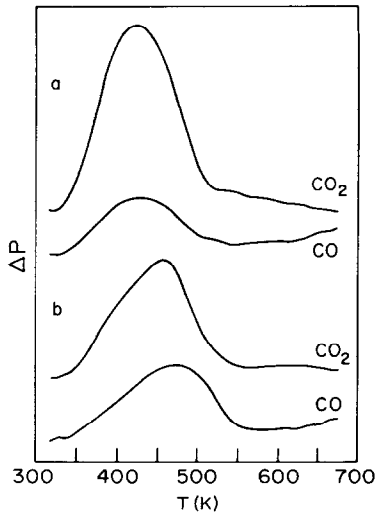

FIG. 5. TPD for CO and O_2 coadsorption on 4.7-nm particles. Results were obtained by (a) adsorbing CO after saturating the surface with O_2 and (b) adsorbing CO following NO TPD without removing oxygen formed by dissociation. The area of the CO_2 peak in (b) is 50% that of (a).

DISCUSSION

In our earlier TPD studies of CO adsorption on Pt and Rh particles supported on α-Al_2O_3, we found that the observed desorption states on small particles could be identified with similar desorption states on single crystals of these metals (*1–3*). Furthermore, correlation of the desorption states on small particles with those observed on single crystals led to the conclusion that changes in adsorption properties with particle size are related to the geometry of the sites. On Pt, CO desorption states on small particles, which would be expected to have many edge and corner atoms with low coordination to the surface, were found to be similar to desorption states found on highly stepped, single crystals. Desorption of CO on larger Pt particles was more similar to that observed on atomically smooth surfaces such as Pt(111). On Rh, TPD results for CO were found to be independent of both particle size and crystal plane, implying that TPD of CO on Rh is not dependent on the surface geometry.

The TPD curves for NO are basically consistent with the idea that changes in adsorption properties with particle size are influenced by changes in site geometry. In studies on Rh single crystals, the temperatures at which molecular NO desorbs and the fraction of NO which dissociates in TPD do not appear to be strong functions of crystal plane (*12–17*). Our results on small particles are very similar and indicate that the NO desorption temperatures and the fraction of NO dissociating in TPD are also not strongly influenced by particle size. However, the desorption temperatures for N_2 are affected by crystal plane on single crystals and correspond to the range of temperatures observed on small particles. As with CO on Pt and Rh, a particle size dependence is only observed when crystal plane dependences are also observed.

The N_2 desorption results, however, also indicate that desorption from small particles probably cannot be considered equivalent to desorption from a sum of simple single-crystal surfaces. On 2.6-nm Rh particles, N_2 desorbs in a single broad peak above 600 K. While absolute peak tempera-

tures are a function of heating rate and this peak may correspond to the 700-K N_2 peak on Rh(100) (*15, 16*), an additional N_2 desorption peak at 450–460 K has been observed on all Rh single crystals that have been studied. Therefore, the reactivity of nitrogen atoms on small Rh particles could not be predicted by modeling small particles as a sum of desorption states on single-crystal surfaces.

The underlying reasons for the differences in N_2 desorption rates between Rh particles and Rh crystals are uncertain. The fact that the N_2 desorption due to atom recombination on Rh(100) occurs at higher temperatures than are observed on Rh(111) or Rh(110) suggests that site symmetry is important. However, whether this is due to increased interactions between adsorbed nitrogen atoms on certain crystal planes, increased N–Rh bond strengths at certain sites, or an increased activation energy for diffusion of the nitrogen atoms cannot be determined at this time.

While many factors can influence desorption rates and we cannot determine which of these is most important, consideration of the observed changes in the N_2 desorption rates can be important in understanding the catalytic activity of Rh catalysts for NO reduction. Oh *et al.* (*10*) developed a kinetic model for NO reduction by CO on Rh(111) which accurately predicted the reaction rates at high pressures. Their model assumed the elementary reaction steps shown below and used rate parameters which were measured elsewhere in TPD experiments under ultrahigh vacuum conditions,

$$CO \rightleftharpoons CO_{ad} \quad (1)$$

$$NO \rightleftharpoons NO_{ad} \quad (2)$$

$$NO_{ad} \rightarrow N_{ad} + O_{ad} \quad (3)$$

$$NO_{ad} + N_{ad} \rightarrow N_2 + O_{ad} \quad (4)$$

$$2\ N_{ad} \rightarrow N_2 \quad (5)$$

$$CO_{ad} + O_{ad} \rightarrow CO_2 \quad (6)$$

More interesting, Oh *et al.* also compared the specific reactivity of Rh(111) to that of a Rh/Al_2O_3 catalyst (average particle size of ~3.5 nm) and found a significantly higher activation energy and a lower specific reaction rate on the supported catalyst. Since our results imply that the desorption rate of N_2 on small particles could be significantly different from that on Rh(111), we examined the effect on the rate of NO reduction by CO of eliminating step (4), associated with N_2 desorption at 450 K, and increasing the activation energy for step (5), the atom recombination step. For these calculations, we have used the reactions and rate parameters from Oh *et al.* for Rh(111), changing only the N_2 desorption activation energy at saturation coverages from 27 to 32.7 kcal/mol and eliminating step (4). The value of 32.7 kcal/mol was calculated from the N_2 peak temperature for 2.6-nm particles assuming that the desorption preexponential remains constant. The results are shown in Fig. 6, along with the rates reported for Rh(111) and the Rh-supported catalyst.

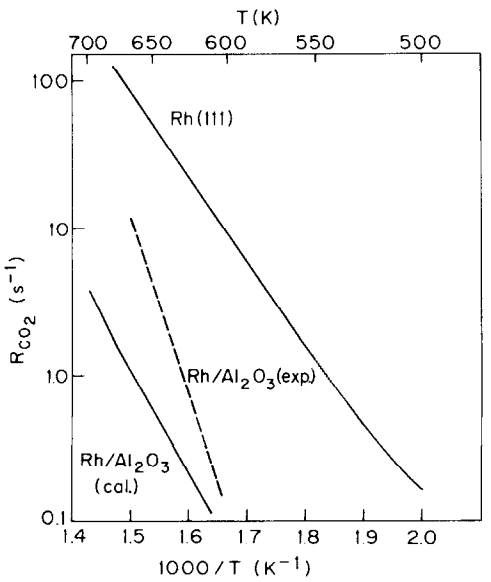

FIG. 6. Rates for NO reduction by CO. Rates on Rh(111) and Rh/Al_2O_3(exp) are from Ref. (*10*), with the calculated results for Rh/Al_2O_3 based on the model in Ref. (*10*) and TPD results for 2.6-nm Rh particles. The line for Rh(111) indicates both measured and predicted reaction rates. For this calculation, P_{CO} and P_{NO} are both 0.01 atm.

While the revised rate model does not accurately predict the rates for the Rh/Al_2O_3 catalyst in absolute terms, the results show the correct trends and imply that the observed changes in N_2 desorption could be responsible for the lower activity of the supported catalyst. According to this, the lower rates on the supported catalyst are due to increased coverages of nitrogen during reaction and the effect of this nitrogen on the adsorption of CO and NO. It is interesting to note that both Auger spectra following reaction and the previous calculations of rates on the Rh(111) surface showed that the surface was indeed covered with nitrogen during reaction (*10*). Changing the activation energy of the nitrogen recombination step, reaction (5), was mainly responsible for lowering the calculated rates. While the elimination of step (4) did not affect the rates significantly at the pressures in Fig. 6, the calculated pressure dependences are changed by the removal of this elementary reaction. Therefore TPD results and the model imply that NO reduction should depend on particle size and that changes in N removal from the surface cause this particle size effect, not changes in NO dissociation kinetics.

SUMMARY

Our results for NO desorption from small particles of Rh on α-$Al_2O_3\{0001\}$ correlate well with results from single crystals of Rh. Only minor differences are observed in studies of various single crystals and in particles ranging in size for both the molecular NO desorption states and the fraction of NO dissociating in TPD; however, more significant differences are apparent for N_2 desorption on both single-crystal and supported particle catalysts. These results are consistent with previous studies which showed that particle size effects are expected when crystal plane dependences are observed (*3*), although desorption of N_2 from NO adsorption on particles does not appear to be just a simple sum of rates from different single crystals. Modeling of NO reduction by CO also implies that these changes in the desorption rates for N_2 could explain the structure sensitivity of this reaction on Rh catalysts.

REFERENCES

1. Altman, E. I., and Gorte, R. J., *Surf. Sci.* **172,** 71 (1986).
2. Altman, E. I., and Gorte, R. J., *J. Catal.* **110,** 191 (1988).
3. Altman, E. I., and Gorte, R. J., *Surf. Sci.*, **195,** 392 (1988).
4. Demmin, R. A., and Gorte, R. J., *J. Catal.* **90,** 32 (1984).
5. Gorte, R. J., *J. Catal.* **75,** 164 (1982).
6. Goodman, D. W., Kelley, R. D., Madey, T. E., and Yates, J. T., Jr., *J. Catal.* **63,** 226 (1980).
7. Kelley, R. D., and Goodman, D. W., *Surf. Sci.* **123,** 743 (1982).
8. Goodman, D. W., *J. Vac. Sci. Technol.* **20,** 522 (1982).
9. Goodman, D. W., *Surf. Sci.* **123,** 679 (1982).
10. Oh, S. H., Fisher, G. B., Carpenter, J. E., and Goodman, D. W., *J. Catal.* **100,** 360 (1986).
11. Hecker, W. C., and Breneman, R. B., "Catalysis and Automotive Pollution Control" (A. Crucq and A. Frennet, Eds.), p. 257. Elsevier, Amsterdam, 1987.
12. Castner, D. G., and Somorjai, G. A., *Surf. Sci.* **83,** 60 (1979).
13. Root, T. W., Schmidt, L. D., and Fisher, G. B., *Surf. Sci.* **134,** 30 (1983).
14. Baird, R. J., Ku, R. C., and Wynblatt, P., *Surf. Sci.* **97,** 346 (1980).
15. Villarubia, J. S., and Ho, W., *J. Chem. Phys.* **87,** 1 (1987).
16. Ho, P., and White, J. M., *Surf. Sci.* **137,** 103 (1984).
17. Bugyi, L., and Solymosi, F., *Surf. Sci.* **188,** 475 (1987).
18. Campbell, C. T., and White, J. M., *Appl. Surf. Sci.* **1,** 347 (1983).
19. Root, T. W., Fisher, G. B., and Schmidt, L. D., *J. Chem. Phys.* **85,** 4679 (1986).
20. Root, T. W., Fisher, G. B., and Schmidt, L. D., *J. Chem. Phys.* **85,** 4687 (1986).
21. Hecker, W. C., and Bell, A. T., *J. Catal.* **84,** 200 (1984).
22. Chin, A. A., and Bell, A. T., *J. Phys. Chem.* **87,** 3700 (1983).
23. Root, T. W., Schmidt, L. D., and Fisher, G. B., *Surf. Sci.* **150,** 173 (1985).
24. Doering, D. L., Poppa, H., and Dickinson, J. T., *J. Vac. Sci. Technol.* **20,** 827 (1982).